Inorganic Chemistry

Article

pubs.acs.org/IC

New Trick for an Old Ligand! The Sensing of Zn(II) Using a Lanthanide Based Ternary Yb(III)-cyclen-8-hydroxyquinoline System As a Dual Emissive Probe for Displacement Assay

Steve Comby,* Sarah A. Tuck, Laura K. Truman, Oxana Kotova, and Thorfinnur Gunnlaugsson*

School of Chemistry, Centre for Synthesis and Chemical Biology and Trinity Biomedical Sciences Institute, Trinity College Dublin, Dublin 2, Ireland

Supporting Information

ABSTRACT: A novel near-infrared (NIR) emissive lanthanide-based zinc sensor was designed, based on the self-assembly in aqueous solution between the nonemissive coordinatively unsaturated Yb(III) cyclen complex **2·Yb** and the sulfonated 8-hydroxyquinoline (**8-HQS**) chromophore, which was employed as a sensitizing antenna. The resulting ternary complex, **2·Yb·8-HQS**, displayed metal-centered emission in the NIR range upon excitation of the antenna with high quantum yield of $Q = 0.23 \pm 0.03\%$ in pH 7.4 buffered aqueous solution; demonstrating efficient sensitization from **8-HQS**. The addition of zinc led to quenching of the NIR emission as a result of the dissociation of the luminescent ternary **2·Yb·8-HQS** complex, where the **8-HQS** antenna was displaced from the Yb(III) center in favor of the formation of more stable chelates with Zn(II). These newly formed Zn(II) complexes were shown to exhibit strong green fluorescence; allowing for the simultaneous sensing of Zn(II) both within the visible and the NIR regions at physiological pH in competitive media. Furthermore, **2·Yb·8-HQS** was shown to be able to detect Zn(II) with good selectivity and in a reversible manner, even in the presence of competitive group (I) and (II) metal ions as well as in the presence of several biologically important d-metal ions.

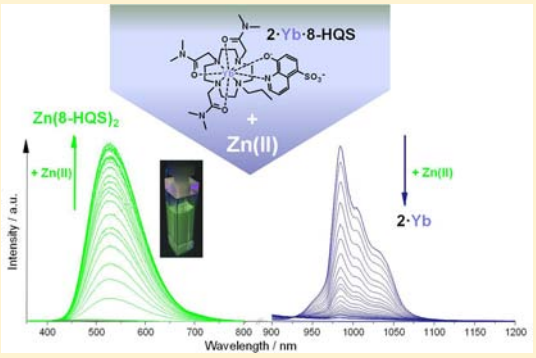

INTRODUCTION

A growing number of diseases have been identified in recent times as arising from metal imbalance in cells and tissues. Hence, a great current interest within the scientific community focuses on the development of novel probes that can selectively identify, quantify, and localize the presence of such metal ions within their native physiological environments.[1] Among transition metal ions, Zn(II), the second most abundant metal ion after Fe(II) in the human body, has been recognized as being extremely important in neurobiology,[1,2] as well as being an essential factor in many biological processes such as brain and immune functions.[1b,3−5] However, abnormal zinc homeostasis has been linked to a growing number of diseases,[6] including different types of cancer[2d,3,7] as well as neurodegenerative disorders characteristic of both Alzheimer's and Parkinson's diseases.[1a,4,8] The growing contributions of zinc homeostasis to neurophysiology and neuropathology have prompted the design and development of numerous fluorescent sensors for the detection of Zn(II) in biological samples.[2,9] These fluorescent probes are usually relatively noninvasive, consisting of organic dyes such as naphthalimide,[10] rhodamine,[2c,9c,11] boron-dipyrromethene (BODIPY),[12] or naphthalene/anthracene[13] that have been further functionalized with chelating receptor units, for instance iminodiacetate, di(2-picolyl)amine, or quinoline moieties, which are able to coordinate Zn(II). Recently, heavy metal complexes such as Ru(II), Pt(II), Ir(III), and Re(I) have also been developed for the sensing and imaging of metal ions as an alternative to organic dyes because of their advantageous photophysical properties and relatively long-lived emission (μs range).[14] Besides the use of transition metal complexes, luminescent lanthanide (Ln) complexes have also been concurrently investigated for the detection of Zn(II)[15−17] and other metal ions.[18] These take advantage of the lanthanides' unique photophysical properties that include easily recognizable line-like emission spectra in the visible region for ions such as Eu(III) and Tb(III), long excited-state lifetimes (μs to ms range), and large Stokes shifts upon ligand excitation, each of these properties being highly desirable for sensing purposes.[19] Recently, the extension to the use of near-infrared (NIR)-emitting lanthanide ions has added another exciting dimension to this field.[20,21] NIR-emitting molecular probes and sensors are particularly interesting as NIR photons allow the exploration of deeper tissues as biological tissues have very low absorption coefficients above 700 nm, with the further advantage of minimizing tissue autofluorescence, which leads to improved signal-to-noise ratios for such sensory systems.[22,23] However, as these are f-f forbidden transitions, the excited state population

Received: April 4, 2012
Published: September 13, 2012

Scheme 1. Formation of the 1:1 Ternary Complex between 2·Yb and 8-HQS

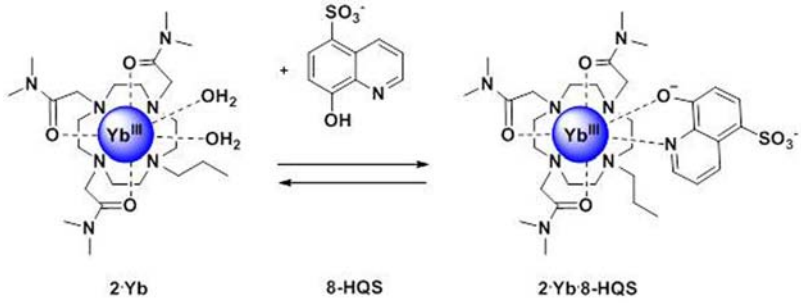

Scheme 2. Synthesis of Ligand 2 and Its Corresponding Yb(III) Complex, 2·Yb

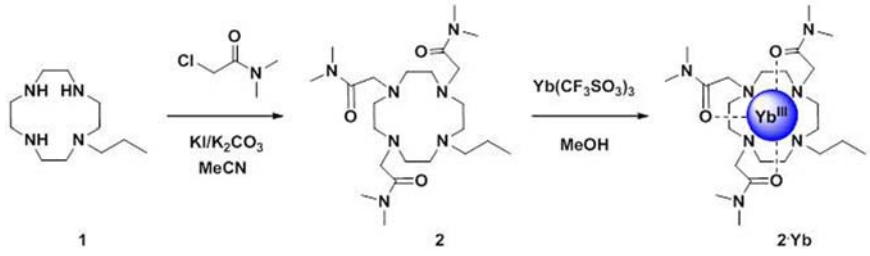

of these lanthanides usually requires the use of sensitizing antennae.[19]

Unlike that developed to date, where visibly emitting Ln(III) based Zn(II) sensors have been covalently functionalized with a targeting Zn(II) chelating unit, our design relies on the formation of a luminescent ternary lanthanide complex and subsequent dissociation of this resulting sensory system upon binding to Zn(II). This approach has previously been used successfully for the sensing of biologically relevant anionic molecules,[24] where the anions bind strongly to the Ln(III) center, concomitantly displacing the sensitizing antenna. Herein, we demonstrated that with a slight modification to this design, by carefully selecting the sensitizing antenna so that it can also bind to d-metal ions, the detection of such ions with high accuracy is achieved by monitoring both the changes in the Ln(III)-centered emission and in the fluorescence arising from the interaction of the metal ions with the sensitizing antennae. Moreover, in our system two different emission channels can be monitored simultaneously, each occurring on a different time frame, in the μs and ns ranges for Yb(III) and Zn(II) chelates, respectively. This makes such sensing highly desirable as it enables for real-time sensing, improving therefore the sensitivity of the detection. However, it is important to point out that this detection/sensing occurs within two separate spectra and on two different time frames (which are three-orders of magnitude different) such sensing cannot be classified as being ratiometric in its nature. The idea presented in this work was first demonstrated using 4,7-diphenyl-1,10-phenanthroline-disulfonate and a visibly emitting Eu(III) cyclen complex for the sensing of Fe(II) in competitive media at physiological pH.[18a] In the present study, we extended this approach toward the use of a NIR-emitting ternary system formed between the nonemissive Yb(III) cyclen complex, **2·Yb**, and the 8-hydroxyquinoline-5-sulfonic acid (**8-HQS**) antenna for the detection of Zn(II) in aqueous solution at physiological pH (Scheme 1). In our novel system, the Yb(III)-cyclen complex, **2·Yb**, has three *N*,*N*-dimethylacetamide arms and a short alkyl chain to avoid the presence of N−H oscillators, which are particularly efficient luminescence quenchers. The **8-HQS** antenna was selected for its ability to strongly bind to Ln(III) ions and to efficiently sensitize their NIR emission via energy transfer from its low-lying triplet excited state.[25−27]

Furthermore, the choice of **8-HQS** has been motivated by the fact that its nonsulfonated analogue, **8-HQ**, was the first fluorescent indicator for the selective detection of Zn(II) in blood plasma and urine.[1a,28] Using our system, we foresaw that the Yb(III)-centered NIR emission of **2·Yb·8-HQS** would be modulated or *switched off* through the displacement of the **8-HQS** antenna in the presence of Zn(II), for which it has high affinity.[29] Concomitantly, the formation of Zn(**8-HQS**)$_x$ (x = 1,2) would give rise to a significant enhancement (*switch on*) of the **8-HQS**-centered emission in the visible region. Herein we give full account of our findings and demonstrate the ability of **2·Yb·8-HQS** to be applied in luminescent displacement assays for the detection of Zn(II) in aqueous solution. Moreover, the influence of pH, as well as other biologically relevant cations and anions on the photophysical properties of **2·Yb·8-HQS** and sensitivity of the Zn(II) detection was also investigated. Finally, we demonstrate that the dissociation of **2·Yb·8-HQS** in the presence of Zn(II), to give Zn(**8-HQS**)$_x$ and **2·Yb** is a reversible process, as upon addition of EDTA the Zn(II) is extracted from Zn(**8-HQS**)$_x$ allowing for the recovery of the luminescent ternary self-assembly **2·Yb·8-HQS** with enhancement in the NIR-centered emission and a concomitant quenching of the fluorescence emission in the visible region.

RESULTS AND DISCUSSION

Synthesis of 2·Yb. The synthesis of **2·Yb** is shown in Scheme 2 and involved the initial formation of the monoalkylated species **1** in 87% yield from the commercially available 1,4,7,10-tetraazacyclododecane, using a synthetic method developed in our laboratory.[30] The alkylation of the remaining three amines was then achieved in acetonitrile using 2-chloro-*N*,*N*-dimethylacetamide in the presence of potassium carbonate and potassium iodide. After purification by column chromatography on neutral alumina (eluting with CH_2Cl_2), **2**

dx.doi.org/10.1021/ic300697w | *Inorg. Chem.* 2012, 51, 10158−10168

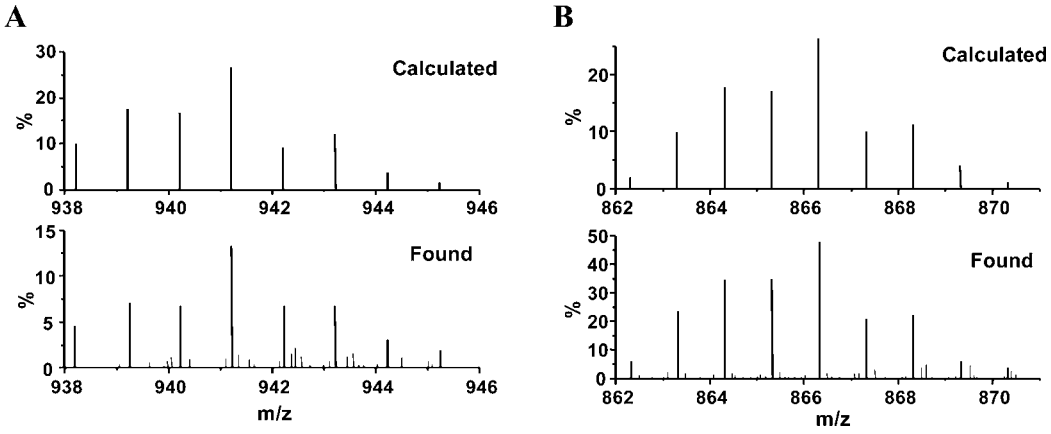

Figure 1. Parts of the MALDI mass spectra of **2·Yb** (10^{-4} M in methanol) in the absence (**A**) and presence of **8-HQS** (**B**) and their corresponding calculated isotopic distribution patterns.

was obtained in 61% yield and fully characterized using conventional methods such as ^{1}H NMR, ^{13}C NMR, and IR (See Supporting Information, Figures S1–S2).

The Yb(III) complex of **2** was formed by microwave irradiation for 40 min in methanol using 1 equiv of $Yb(CF_3SO_3)_3$, giving **2·Yb** in 81% yield. The successful formation of the desired product was confirmed by ^{1}H NMR analysis (Supporting Information, Figure S3) as well as by means of high resolution mass spectrometry (HRMS), which showed that the isotopic distribution pattern matched that of the calculated species, Figure 1A, and by using IR (Supporting Information, Figure S4), where a shift in the carbonyl signals (by ~20 cm^{-1}) indicated the coordination of the carbonyl groups to the Yb(III) center.

Formation and Photophysical Characterization of 2·Yb·8-HQS in Solution. Having successfully synthesized **2·Yb**, the formation of the ternary complex **2·Yb·8-HQS** in solution was first investigated by using HRMS, where solutions of **2·Yb** (10^{-4} M), in the absence and presence of 1.2 equiv of **8-HQS**, were prepared and analyzed using MALDI-MS. The results from these measurements are shown in Figure 1 A and B, respectively, and demonstrated that, in the absence of **8-HQS**, a m/z peak corresponding to a +1 charged species was observed with a m/z = 941.2256, which was assigned to [**2·Yb** + $2CF_3SO_3^-$]$^+$; conversely, analysis of the solution containing **8-HQS** revealed the presence of a single charged species at m/z = 866.3179, corresponding to the ternary complex [**2·Yb·8-HQS**]$^+$. In both cases, as it is evident from Figure 1, the isotopic distribution patterns were shown to match those of the calculated spectra.

We next investigated the formation of the ternary complex in solution by probing the changes in the absorption spectrum of the **8-HQS** antenna in HEPES buffered solution. At pH 7.4, the UV–visible absorption spectrum of **8-HQS** displays two main bands centered at 240 and 310 nm. These were assigned to the $\pi\rightarrow\pi^*$ and $n\rightarrow\pi^*$ transitions of **8-HQS**; and according to published pK_a values for **8-HQS** (p$K_{a,\ \text{quinoline}}$ = 3.93; p$K_{a,\ \text{hydroxyl}}$ = 8.42),[26a,29,31,32] correspond to the monodeprotonated form of **8-HQS**. Further deprotonation of the hydroxyl group, or binding to a metal ion results in a significant red shift for both of these bands (Supporting Information, Figure S5A).[32] This is particularly useful for monitoring the formation of the ternary complex between **2·Yb** and **8-HQS** in solution, as it enables a clear distinction between the free and bound antenna. Indeed, this was found to be the case, as when a pH 7.4 HEPES buffered solution of **2·Yb** (5×10^{-5} M) was titrated with **8-HQS**, the formation of new absorption bands at 255 and 365 nm, characteristic of the bound antenna, were observed. Here, the most significant changes occurred between the addition of 0→1 equiv of **8-HQS**, Supporting Information, Figure S5B. Concomitantly, the absorption bands of the free antenna, centered at 240 and 310 nm, showed a reverse trend; with larger enhancement in the absorbance after the addition of 1 equiv of **8-HQS**; indicating the formation of the 1:1 ternary complex between **2·Yb** and **8-HQS**.

As **8-HQS** is known to be an efficient sensitizer for NIR-emitting Ln(III) ions,[25–27] the formation of **2·Yb·8-HQS** in situ was also monitored by observing the appearance of the Yb(III)-centered emission upon binding of **8-HQS** to **2·Yb** under the same experimental conditions as above. In the absence of any chromophoric group able to act as an antenna and in the presence of two metal bound water molecules,[24] the metal-centered emission of the **2·Yb** cyclen complex was found to be extremely weak. However, upon titration with **8-HQS**, the appearance of the characteristic Yb(III)-centered NIR luminescence between 920 and 1100 nm was observed upon antenna excitation at 360 nm, Figure 2. The Yb(III) emission displayed a sharp main component at 985 nm and broader components at longer wavelengths due in part to vibronic transitions. The changes observed in the Yb(III) $^2F_{5/2}\rightarrow{}^2F_{7/2}$

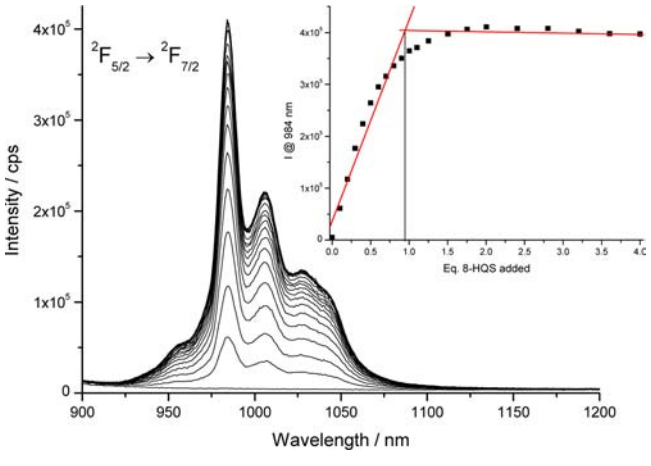

Figure 2. Evolution of the Yb(III) NIR emission (λ_{ex} = 360 nm) of **2·Yb** (5×10^{-5} M) in HEPES buffer upon addition of **8-HQS**.

dx.doi.org/10.1021/ic300697w | Inorg. Chem. 2012, 51, 10158–10168

transition at 984 nm as a function of **8-HQS** concentration confirmed the formation of **2·Yb·8-HQS** in a 1:1 stoichiometry, which implies the direct coordination of the **8-HQS** antenna to the lanthanide ion as no significant emission changes occurred after the addition of 1 equiv of the antenna (see inset in Figure 2). Direct coordination of the quinolinate antenna to the Yb(III) ion of **2·Yb** was further established by measuring the lifetimes of the Yb($^2F_{5/2}$) excited state in the presence of **8-HQS**. Using the empirical equation reported by Faulkner and collaborators[33] and the lifetimes measured in H_2O (3.4 μs) and D_2O (6.1 μs), the hydration state or q value for **2·Yb** was found to be q = 0, indicating the absence of any metal-bound water molecules and thus corroborating the formation of the covalently bound **2·Yb·8-HQS** species.

The changes in the UV−visible absorption and Yb(III) emission were further analyzed by fitting the relative spectroscopic changes using the nonlinear regression analysis program SPECFIT, from which the binding constant for the formation of **2·Yb·8-HQS** was determined as log K_{11} = 5.5 ± 0.3 (See Supporting Information, Figure S6). The energy transfer from the **8-HQS** antenna to the Yb(III) ion is expected to take place via intraligand charge transfer (ILCT) triplet excited states as such excited states, in addition of their well-matched energies with NIR-emitting Ln(III) emitting states,[25−27] have been demonstrated to coexist at room temperature (r.t.) with a ^{1}ILCT singlet state in Gd(III) complexes formed with quinolinate ligands.[34] The sensitization of the NIR emission was conclusively ascertained by the excitation spectra which closely matched the absorption spectra (Supporting Information, Figure S7). Interestingly, the two main bands observed in the excitation spectrum were centered at 255 and 360 nm, indicating that the sensitization of the NIR luminescence only occurs from antennae that are directly coordinated to the Yb(III) ion. Hence, any unbound or excess **8-HQS** would not be expected to contribute to the sensitization process as shown in the inset of Figure 2. This observation seems to demonstrate that the sensitization of the Yb(III)-centered emission occurs from the triplet excited state of the **8-HQS** antenna via a Dexter mechanism, the latter being strongly distance-dependent.[35]

To quantify the ability of **8-HQS** to sensitize the NIR-emitting Yb(III) ion, the quantum yield of **2·Yb·8-HQS** (formed in situ by mixing **2·Yb** and **8-HQS** in a 1:1 stoichiometric ratio, in HEPES pH 7.4 buffered solutions) was determined upon excitation of the antenna. The quantum yield, calculated relative to [Yb(**tta**)$_3$phen] when measured in toluene,[36] was determined as 0.23 ± 0.03%, which is sizable compared to the published literature data,[20,21d,e] particularly in aqueous solution, where the presence of proximate O−H oscillators often induces considerable quenching of NIR-emitting Ln(III) ions. Despite this relatively high quantum yield, it has to be stressed that the Yb(III)-centered NIR emission was also accompanied by some weak ligand-centered fluorescence occurring in the visible range (centered at 495 nm), as a result of an enhancement in the **8-HQS** fluorescence upon binding to the Yb(III) center of **2·Yb**, Supporting Information, Figure S8. The presence of both ligand- and metal-centered emission indicates that even if the sensitization of the $^2F_{5/2}$ excited state of Yb(III) via the antenna is significant, the energy transfer from the antenna to the Ln(III) ion is not complete.

Luminescent Displacement Assay for the Detection of Zn(II) in Aqueous Solution Using 2·Yb·8-HQS. Having established the self-assembly of the 1:1 ternary complex **2·Yb·8-HQS** in buffered solution, we next evaluated the ability of this system to act as a luminescent sensor for Zn(II). The addition of $Zn(ClO_4)_2$ to **2·Yb·8-HQS** (5×10^{-5} M) at pH 7.4 resulted in a significant quenching in the Yb(III)-centered emission of **2·Yb·8-HQS**, with about 95% quenching observed within the addition of 4 equiv of Zn(II), Figure 3. Analysis of these

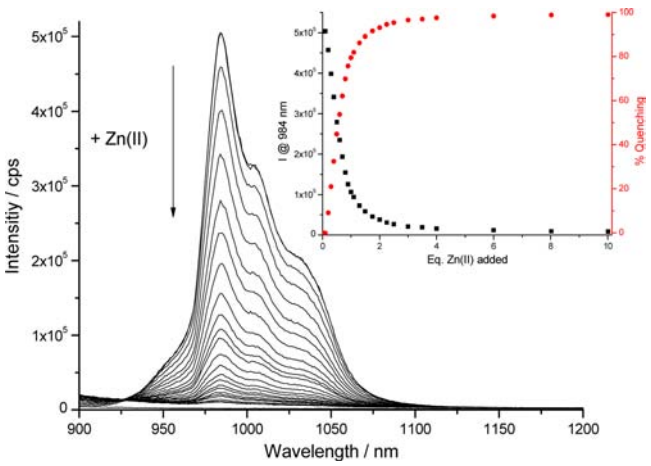

Figure 3. NIR emission spectrum (λ_{ex} = 360 nm) of **2·Yb·8-HQS** (5×10^{-5} M) in HEPES buffer upon titration with Zn(II). Inset: The changes in emission intensity at 984 nm (black squares) and the percentage quenching (right y-scale, red circles) vs the equivalents of Zn(II) added.

changes as a function of added Zn(II) is shown as an inset in Figure 3, and demonstrated that the NIR emission was about 80% quenched after the addition of 1 equiv of Zn(II). The quenching mechanism here involves the Zn(II)-induced displacement of the **8-HQS** antenna from the Yb(III) center (and hence, the dissociation of the luminescent **2·Yb·8-HQS** ternary complex) with the concomitant formation of Zn(**8-HQS**)$_x$ (x = 1,2) chelates. The formation of Zn(II) chelates with **8-HQS** was fully supported by the appearance of an intense and broad quinolinate-based ^{1}ILCT singlet excited state emission centered at 529 nm (Figure 4A and Supporting Information, Figure S9).[37]

The formation of the **8-HQS** Zn(II) complexes impairs the photoinduced charge transfer from the oxygen atom to the pyridinium ring, which, accompanies tautomerization, leading to fluorescence quenching in the free **8-HQS**.[38,39] Assuming that the **8-HQS** fluorescence emission enhancement arises only from the chelation to Zn(II), the quenching in the NIR emission should correspond to the mirror image of the enhancement seen in the visible region. And indeed, this was found to be the case, as is evident from Figure 4B, as upon addition of Zn(II) to a solution of **2·Yb·8-HQS**, the quenching observed in the NIR emission was accompanied by an enhancement in the visible fluorescence which occurred mostly between 0 → 1 equiv of Zn(II), mirroring the changes seen in the Yb(III) emission. The absence of any changes (apart from a loss in intensity) in the excitation spectrum monitored at 985 nm ($^2F_{5/2}$→$^2F_{7/2}$ transition) corroborates the fact that the NIR quenching is purely the result of the antenna displacement and that no other quenching or sensitization mechanisms are taking place during the titration, Supporting Information, Figure S10).

The emission changes observed in both the visible and in the NIR regions as a function of Zn(II) were fitted using nonlinear

dx.doi.org/10.1021/ic300697w | Inorg. Chem. 2012, 51, 10158−10168

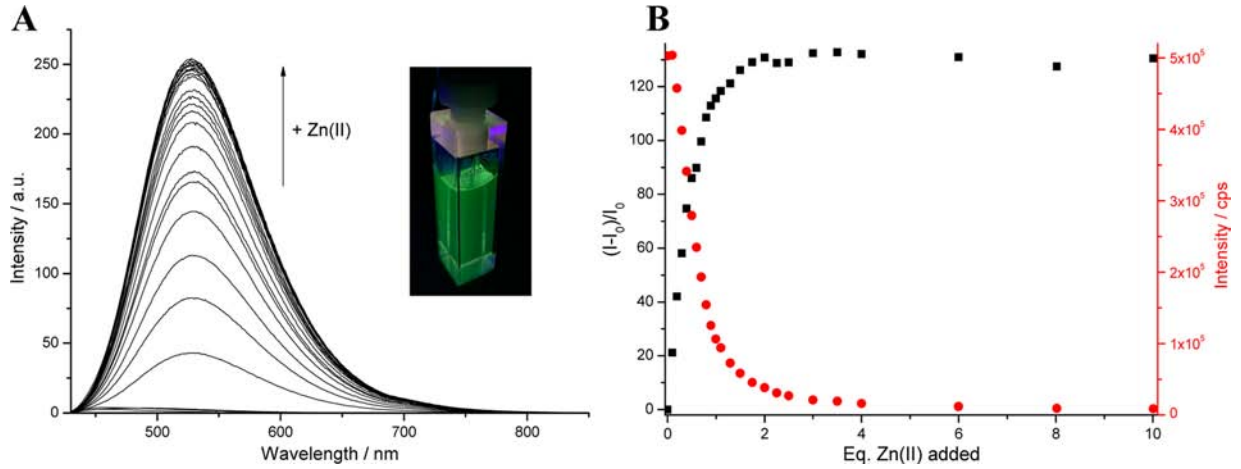

Figure 4. (**A**) Evolution of the fluorescence emission spectrum (λ_{ex} = 360 nm) of **2·Yb·8-HQS** (5×10^{-5} M) in HEPES buffer upon titration with Zn(II). Inset: The emission arising from a solution of **2·Yb·8-HQS** in the presence of Zn(II) under a UV–visible lamp (λ_{ex} = 365 nm). (**B**) The fluorescence enhancement, $(I - I_0)/I_0$, observed in the visible region (black squares) and the concomitant quenching of the Yb-centered NIR emission (right y-scale, red circles) vs the equivalents of Zn(II) added.

regression analysis to determine the conditional stability constants for the formation of the Zn(II) chelates with **8-HQS**. The experimental binding isotherms and corresponding fits at different wavelengths as a function of the Zn(II) concentration are shown in Supporting Information, Figure S11, while the stability constants determined have been summarized in Table 1.

Table 1. Conditional Stability Constants for the M:L 1:1 and 1:2 Zn(II) Chelates Formed after Displacement of 8-HQS from the 2·Yb cyclen Complex and Comparison to the Values Found in the Literature

Zn:**8-HQS**		log K_{11}	log β_{12}
from lit.[a]		7.54	14.32
from UV–visible absorption data[b]		6.4 ± 0.1	12.5 ± 0.2
from fluorescence data[b]	visible	6.65 ± 0.05	12.0 ± 0.2
	NIR	6.87 ± 0.05	11.7 ± 0.1

[a]Taken from ref 29. [b]This work.

The binding constants obtained for the 1:1 Zn(II):**8-HQS** chelates were in relatively good agreement with the values observed in the literature for the formation of such complexes.[29] However, lower binding constants were determined for the 1:2 Zn(II):**8-HQS** chelates, which can be explained by the experiment type used to determine these constants as the competition between **2·Yb** and Zn(II) for **8-HQS** tends to hinder the formation of bis-quinolinate complexes Zn(**8-HQS**)$_2$.

Having demonstrated that Zn(II) can be sensed via a luminescent displacement assay using **2·Yb·8-HQS**, the detection limit for this recognition process was determined by monitoring the NIR emission upon excitation of the **8-HQS** antenna at 360 nm. Here, the quenching in the NIR emission of **2·Yb·8-HQS** (5×10^{-5} M) in 0.1 M HEPES buffer at pH 7.4 revealed a linear relationship within the concentration range [Zn(II)] = 0 →4.5×10^{-5} M (R^2 = 0.983). From these changes, the detection limit (3σ) was calculated and found to be 6.8×10^{-6} M, which compared well with the data published by Hanaoka et al. for the detection of Zn(II) using Tb(III)-based responsive probe.[17a]

The addition of $Zn(ClO_4)_2$ to a solution of **2·Yb·8-HQS** at pH 7.4 also caused significant changes in the absorption spectra of **8-HQS** (Supporting Information, Figures S9 and S12), with a marked hyperchromism being observed for the absorption bands at 255 nm (+70%) and 364 nm (+50%) and a simultaneous hypochromism in the bands at 240 nm (−32%) and 310 nm (−46%). These changes were further accompanied by the appearance of three distinct isosbestic points at 244, 267, and 333 nm, confirming the binding of Zn(II) to **8-HQS**, with stability constants similar to those determined from the emission data, Table 1 and Supporting Information, Figure S12. The sensing of Zn(II) was also investigated in the presence of several anions that are found in high concentrations in biological media, such as carbonate (30 mM), lactate (2.3 mM), citrate (0.13 mM), and phosphate (0.90 mM). While no significant changes were seen in either the ligand or the metal-centered emission of **2·Yb·8-HQS** in the presence of citrate and phosphate, the quenching of the Yb(III)-centered emission was increased in the presence of carbonate and lactate (Supporting Information, Figure S13). This behavior was somewhat expected as, at such high anion concentrations, competition of the anion for the **2·Yb** cyclen complex can possibly lead to partial displacement of the **8-HQS** antenna with concomitant quenching of the Yb(III)-centered emission, without considerably affecting the ligand-centered fluorescence.

*Interaction of **2·Yb·8-HQS** with H^+ and Other d-Metal (Co, Ni, Cu, Cd) or Alkali Metal (Ca, Mg) Ions.* Having demonstrated the Zn(II) sensing ability of **2·Yb·8-HQS** in buffered aqueous solution, we next investigated its behavior as a function of pH, by monitoring the changes in the UV–visible absorption and the emission spectra in both visible and NIR regions within pH 2–10 range. The UV–visible absorption spectrum of the 1:1 solution showed initially a decrease in the lowest energy absorption band around 360 nm as the deprotonation of the quinoline nitrogen was taking place and then, from pH 5, a significant increase, confirming the formation of 1:1 ternary complex between **8-HQS** and **2·Yb** (See Supporting Information, Figure S14A). The behavior of the absorption at higher pH values tends to confirm that the ternary complex was not dissociated at such a pH as the ratio between the bands at 360 and 308 nm remained unchanged. The NIR Yb(III) emission of the 1:1 **2·Yb·8-HQS** complex was

dx.doi.org/10.1021/ic300697w | Inorg. Chem. 2012, 51, 10158–10168

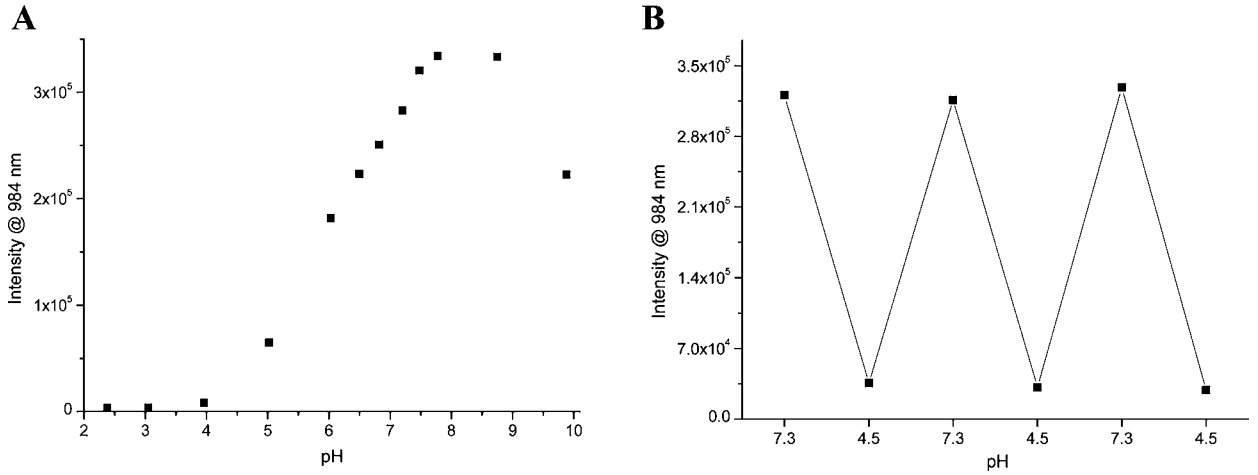

Figure 5. (A) Effect of the pH on the metal-centered emission intensity of a 1:1 **2·Yb·8-HQS** solution in 0.1 M NaCl; [**2·Yb**] = [**8-HQS**] = 5×10^{-5} M, λ_{ex} = 360 nm and λ_{an} = 984 nm. (B) Reversibility of the ON-OFF switching behavior of the metal-centered emission as a function of the pH.

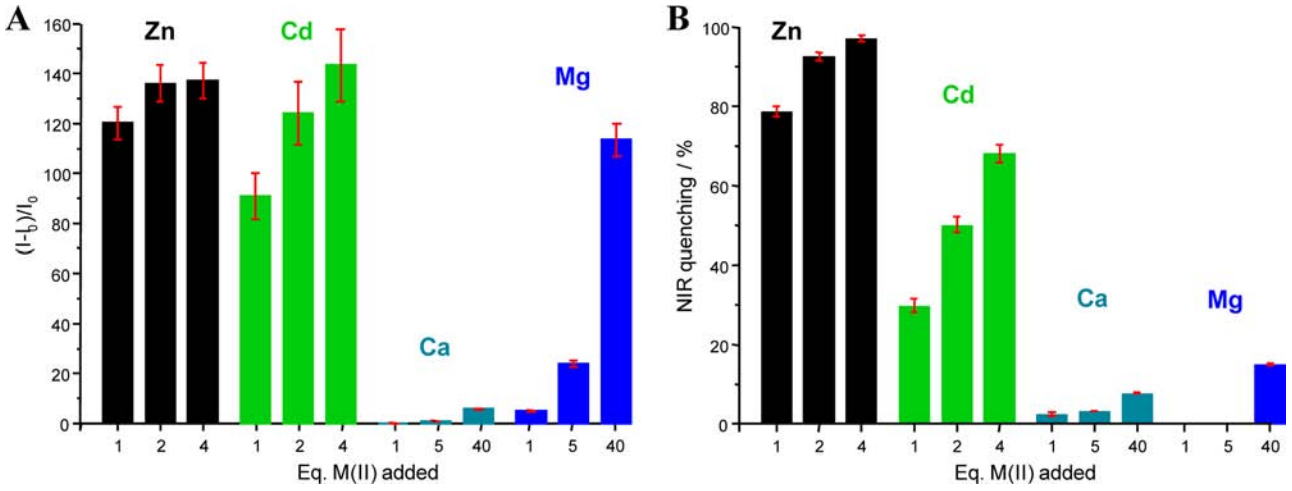

Figure 6. Bar chart diagram representing the ligand-centered fluorescence enhancement (**A**) and the metal-centered NIR emission quenching, in %, (**B**) observed upon addition of Zn(II), Cd(II), Ca(II), and Mg(II) to a **2·Yb·8-HQS** solution in HEPES buffer at pH 7.4; [**2·Yb·8-HQS**] = 5×10^{-5} M, [M(II)] = 0→0.2 mM (M = Zn, Cd) and 2 mM (M = Ca, Mg).

also examined as a function of pH upon excitation at 360 nm and the results demonstrated that for pH ≤ 4, no or very weak NIR emission was observed, Figure 5. This behavior can be explained by the fact that the quinoline nitrogen (pK_a = 3.93)[26a,29] is mainly in its protonated form and therefore prevents the formation of the desired ternary complex and subsequently sensitization of the metal-centered emission.

However, further increase in pH resulted in the steady appearance of the NIR emission (*switch on* effect); reaching a maximum 40-fold luminescence enhancement at pH 7.5. After this pH, the emission at 984 nm remained unchanged until pH 9 before decreasing at higher pH, which is the result of changes in the Yb(III) coordination environment as a function of pH as recently demonstrated for simple cyclen complexes,[40] which in the current case, appears to be detrimental to the sensitization process. As expected from theoretical investigations, the **8-HQS**-centered fluorescence remained weak throughout the titration as the nonemitting zwitterionic species, where the quinoline is protonated, and the hydroxyl group, deprotonated, has been shown to be the most stable excited state form in a wide range of pHs.[39,41] However, a 2-fold enhancement was observed at pH 5 as a result of the binding of **8-HQS** to the Yb(III) metal center, Supporting Information, Figure S15A. This enhancement was then followed by a slight decrease of about 15−25%, within the pH range 5−7.5; a phenomenon that we explain by the increasing efficiency in the NIR sensitization process by the **8-HQS** antenna (as is evident in Figure 5A).

Having established the pH dependence of both NIR and visible emission, we next evaluated the pH-dependent reversibility of the NIR emission as the pH was modulated between pH 7.3 and pH 4.5. As demonstrated in Figure 5B, the NIR emission could be switched reversibly *on* and *off* over several cycles without any indication of signal loss. The reversibility of the system after each pH adjustment was further established by monitoring the changes observed in both the UV−visible absorption and fluorescence spectra of **8-HQS** as a consequence of the formation and subsequent dissociation of the ternary complex **2·Yb·8-HQS** (Supporting Information, Figure S14B and S15B, respectively).

The selectivity of **2·Yb·8-HQS** toward transition metal ions such as Cd(II), Co(II), Ni(II), and Cu(II) at pH 7.4 was also examined by evaluating the changes in the absorption, fluorescence and NIR emission. While each of these metal

dx.doi.org/10.1021/ic300697w | *Inorg. Chem.* 2012, 51, 10158−10168

ions led to a different degree of quenching in the NIR emission, with Cu(II) being the most effective (Supporting Information, Figure S16), only Cd(II) gave rise to an enhancement of the ligand-centered fluorescence in the visible range. For all the other transition metal ions investigated, the ligand-centered fluorescence was further weakened or quenched (Supporting Information, Figures S17−S18). This result particularly emphasized the considerable advantage of having a dual emissive (or two channels) probe in such a displacement assay as, in this case, a clear distinction can be made between the recognition of Zn(II) and Cd(II) (see further discussion below), and that these can be further distinguished from other transition metal ions since their chelation to **8-HQS** antenna gave a selective enhancement in the ligand-centered fluorescence, Figures 4 and Supporting Information, Figure S18. The formation of a metal chelate between Cd(II) and **8-HQS** was further evidenced by the evolution of the UV−visible absorption spectrum of **2·Yb·8-HQS** upon addition of Cd(II). However, Cd(II) resulted in a lower fluorescence enhancement than for Zn(II) (Figure 6A) and the **8-HQS** fluorescence maximum was also slightly less red-shifted upon chelate formation, with a λ_{max} at 524 nm compared to 530 nm for Zn(II), Supporting Information, Figure S19.

The distinction between Zn(II) and Cd(II) was considerably emphasized by analyzing the quenching of the Yb(III)-centered NIR emission as the latter was much less affected by the addition of Cd(II) than Zn(II), Figure 6B. Indeed, while more than 10 equiv of Cd(II) were required to quench 90% of the emission of **2·Yb·8-HQS**, only 1.5 equiv of Zn(II) resulted in the same degree of quenching, Supporting Information, Figure S20. These results altogether are in a good agreement with the stability constants for the formation of the different **8-HQS** metal chelates; with the constants determined for Zn(II) being almost 1 order of magnitude larger than that determined for Cd(II).[29] While the divalent transition metals tested appeared to interfere to some degree with the detection of Zn(II) in aqueous solution, it has to be stressed that these metal ions are not present in micromolar concentrations in typical biological samples and therefore should not limit the use of our system in a variety of applications. To evaluate this, the Zn(II) sensing was investigated in the presence of biologically abundant cations, such as Na(I), Ca(II), and Mg(II), that can be easily found in mM concentrations in biological media. As shown in Figure 7, the presence of both Ca(II) and Mg(II) did not affect the detection of Zn(II), even though some quenching was observed in the NIR emission (<8% for Ca(II) and 15% for Mg(II)) at high concentrations of these ions prior to Zn(II) addition, Figures 6B and Supporting Information, Figure S21).

The partial displacement of the **8-HQS** antenna after the addition of 40 equiv of alkali metal ions was further confirmed by monitoring the changes observed in both the UV−visible absorption and the ligand-centered fluorescence spectra (Supporting Information, Figure S22). Altogether, these measurements clearly demonstrated that Mg(II) binds stronger to **8-HQS** than Ca(II), but that the stability of the ternary complex, **2·Yb·8-HQS**, remained larger than the ones determined for the **8-HQS** chelates formed with either Ca(II) or Mg(II).[29] Whereas only a small percentage of the antenna is displaced in the presence of high concentrations of Ca(II) and Mg(II) (2 mM), the stronger fluorescence of the metal chelates formed prevailed over the very weak ligand-centered fluorescence of the major species in solution, namely, **2·Yb·8-HQS**, leading therefore to a significant enhancement in the

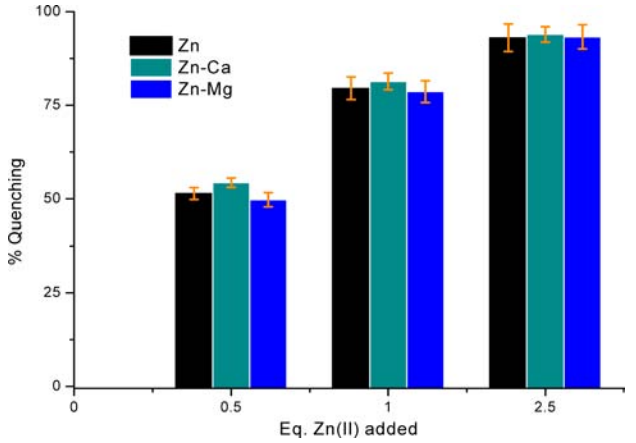

Figure 7. Quenching of the NIR emission, in %, observed upon addition of Zn(II) in the absence and presence of Ca(II) or Mg(II) at a concentration of 2 mM (Errors are given as $\pm 2\sigma$).

emission accompanied with a 14−18 nm red shift (Supporting Information, Figures S22B and S23). However, as soon as Zn(II) was added, both the absorption and the fluorescence spectra displayed further changes to match finally the spectra shown in Figure 4 and Supporting Information, Figure S12.

Reversibility Studies. Having demonstrated that the formation of the ternary complex was fully reversible as a function of the pH, it was important to show that the sensing of Zn(II) could be as well reversed. To demonstrate this, a solution of **2·Yb·8-HQS** in pH 7.4 buffer was first titrated with Zn(II) (0→10 equiv), followed by the addition of EDTA. As shown in Figure 8, the addition of EDTA led to the complete dissociation of the Zn(**8-HQS**)$_x$ (x = 1,2) chelates and, consequently, the loss of the ligand-centered fluorescence. This was associated with a full recovery of the metal-centered NIR emission, confirming the reformation of **2·Yb·8-HQS**. This behavior, further confirmed by UV−visible absorption (Supporting Information, Figure S24), is particularly interesting as it would allow for both direct and indirect determination of the Zn(II) as well as multisampling possibilities.

CONCLUSION

In this work, the photophysical properties of the luminescent **2·Yb·8-HQS** ternary complex obtained through the self-assembly between the **2·Yb** cyclen complex and the sensitizing 8-hydroxyquinoline antenna, **8-HQS**, were investigated in aqueous solution at physiological pH in the presence of Zn(II) and other biologically relevant metal ions. First, we have demonstrated, using different spectroscopic techniques, that **8-HQS** can associate strongly with the newly designed Yb(III) cyclen complex in a 1:1 stoichiometry with a log K of 5.5 ± 0.3. The resulting 1:1 ternary complex displayed sizable metal-centered NIR emission (Q = 0.23 ± 0.03) upon excitation into the absorption bands of the **8-HQS** antenna. Monitoring the excitation spectra (at the maximum Yb(III) emission intensity) confirmed the sensitization by **8-HQS**, as well as demonstrated that the energy transfer from the antenna to the Yb(III) ion occurred only when the former was bound to **2·Yb**.

Addition of Zn(II) to this ternary system resulted in a complete quenching of the metal-centered NIR emission, which was accompanied by a significant enhancement of the ligand-centered visible fluorescence. This behavior we explained by the displacement of the antenna from the Yb(III) cyclen complex

dx.doi.org/10.1021/ic300697w | *Inorg. Chem.* 2012, 51, 10158−10168

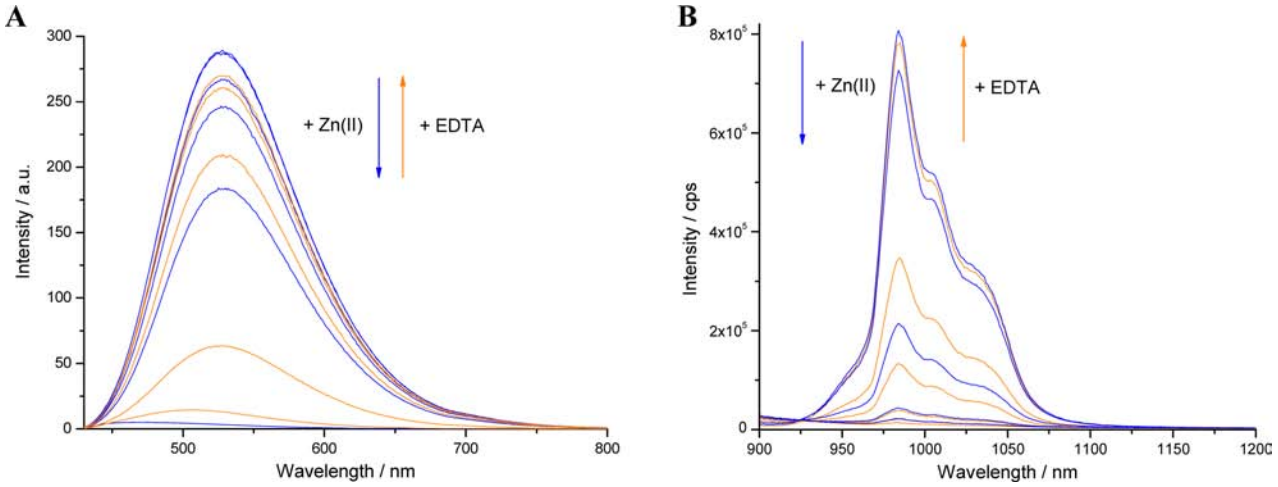

Figure 8. Evolution of the fluorescence (A) and NIR emission (B) of **2·Yb·8-HQS** (5×10^{-5} M) in HEPES buffer upon titration with Zn(II) (blue curves; 0→10 equiv) followed by the addition of EDTA (orange curves; 0→10 equiv).

and concomitant formation of the Zn(II) chelates with **8-HQS**. Using this system, we were able to achieve a limit of detection of 6.8 μM for Zn(II) at pH 7.4 and to show that the presence of biologically relevant anions, while not influencing the ligand-centered fluorescence, had a more marked effect on the Yb(III)-centered emission. This was particularly noticeable in the case of carbonate and lactate. The response of **2·Yb·8-HQS** toward cations such as Cd(II), Co(II), Ni(II), Cu(II), Ca(II), and Mg(II) as well as the pH was also investigated. The self-assembly of the ternary complex was shown to be fully reversible (*OFF-ON* switching) as a function of the pH, reaching its maximum NIR emission intensity between pH 7 and 9. While divalent transition metal ions, such as Ni(II), Co(II), and Cu(II) do interfere to some degree with the sensing of Zn(II), with Cu(II) leading to the larger quenching in the NIR emission, none of them resulted in an enhancement of the ligand-centered fluorescence. This result emphasized the importance of having a dual emissive probe (or a dual channel), emitting in completely different ranges of the electromagnetic spectrum, as this allows to differentiate Zn(II) from other divalent transition metal ions. It is noteworthy here to stress that this displacement assay is not an example of ratiometric sensing as the emission changes occur at two different time frames, originated from two different species, that is, the formation of the Zn(**8-HQS**)$_x$ (x = 1,2) chelates and the concomitant dissociation of the ternary **2·Yb·8-HQS** system. However, both can be used, as we have demonstrated, independently to monitor the Zn(II) sensing.

The detection of Zn(II) was also evaluated in the presence of Ca(II) and Mg(II) and showed little or no influence in the presence of such ions, even at a concentration as high as 2 mM. Finally, the response of **2·Yb·8-HQS** to the presence of Zn(II) was shown to be fully reversible upon addition of EDTA, opening perspectives for multiple detection analysis.

EXPERIMENTAL SECTION

Starting Materials and General Procedures. All solvents and chemicals were purchased from commercial sources and used without further purification. 1,4,7,10-Tetraazacyclododecane (cyclen) and HEPES buffer (titration, ≥ 99.5%) were purchased from CheMatech and Sigma, respectively, while 8-hydroxyquinoline (8-HQ) was from May and Baker Ltd. $MCl_2 \cdot xH_2O$ (M = Cd(II), Ca(II), Mg(II), Cu(II), Co(II) with x = 0, 2, 4 or 6), $FeCl_3 \cdot 6H_2O$, and $Zn(ClO_4)_2 \cdot 6H_2O$ were purchased either from Sigma, Aldrich or BDH Ltd., Poole, England. Water was purified using a Millipore Milli-Q water purification system. Ethylenediaminetetraacetic acid (EDTA) solution 0.0104 M in water was purchased from Fluka. The HEPES buffer solution was prepared by dissolving 4-(2-hydroxyethyl)piperazine-1-ethanesulfonic acid (HEPES, 0.1 M) and NaCl (ionic strength) in Millipore water before the pH was adjusted to 7.4 with NaOH. ^{1}H- and ^{13}C NMR spectra were recorded in chloroform-*d* (>99.8 atom % D) and dimethyl-d_6 sulfoxide (>99.8 atom % D) from Apollo Scientific Ltd. using a Bruker Spectrospin DPX-400 spectrometer. Chemical shifts are reported in ppm using deuterated solvents as internal standards. Mid-infrared spectra were recorded using a Perkin-Elmer Spectrum One FT-IR spectrometer equipped with a universal attenuated total reflection (ATR) sampler. Mass spectrometry was carried out using HPLC grade solvents. Electrospray mass spectra (ES-MS) were measured on a Micromass LCT spectrometer calibrated using a leucine enkephaline standard. MALDI Q-Tof mass spectra were carried out on a MALDI Q-Tof Premier (Waters Corporation, Micromass MS technologies, Manchester, U.K.) and high-resolution mass spectrometry was performed using Glu-Fib as an internal reference (peak at m/z 1570.6774). Thermogravimetric analysis (TGA) of **8-HQS** was obtained using a Perkin-Elmer Pyrus 1 TGA instrument. Elemental analyses were performed by the Microanalytical Laboratory of the University College Dublin.

8-Hydroxyquinoline-5-sulfonic Acid (8-HQS). 8-Hydroxyquinoline-5-sulfonic acid was synthesized according to the literature procedure.[42] Briefly, 1.020 g of 8-hydroxyquinoline (7.0 mmol) was placed in a round-bottom flask and covered with a minimum of oleum (H_2SO_4, SO_3 20%). The mixture was stirred at r.t. overnight and poured over ice, yielding a precipitate, which was filtrated and washed with cold water. The solid collected was dried under vacuum to give a yellow powder (1.710 g, 100% yield). ^{1}H NMR (400 MHz, dmso-d_6): δ = 12.11 (s, 1H, OH), 9.77 (d, 1H, J = 8.7 Hz, ArH_a), 9.09 (d, 1H, J = 5.2 Hz, ArH_b), 8.15−8.11 (dd, 1H, J = 5.2 Hz, ArH_c), 8.08 (d, 1H, J = 8.0 Hz, ArH_d), 7.33 (d, 1H, J = 8.0 Hz, ArH_e). ES-MS (ES^+) Calculated for $C_9H_7NO_4SNa$ $[M + Na]^+$: m/z = 247.9994, found: m/z = 247.9997. IR υ_{max} (cm^{-1}): 3391 (s, O−H stretch), 3080 (m, C−H aromatic), 1552 (s, C═C aromatic), 1383 (s, ring stretching), 1181 (s, C−O stretch). TGA of **8-HQS** powder sample was used to determine the water content and showed the presence of one water molecule that has been taken into account in the molecular weight for all the **8-HQS** solutions prepared. Elemental analysis calculated for $C_9H_7NO_4S \cdot 0.8$ $H_2O \cdot 0.1$ H_2SO_4: C, 43.34; H, 3.56; N, 5.62; Found: C, 43.16; H, 3.25; N, 5.58.

1-Propyl-1,4,7,10-tetraazacyclododecane (1). 1-Bromopropane (0.260 mL, 2.9 mmol, 1.0 equiv) was added to a $CHCl_3$ solution of 1,4,7,10-tetraazacyclododecane (2.000 g, 11.6 mmol, 4.0 equiv) and freshly distilled NEt_3 (0.480 mL, 3.5 mmol, 1.2 equiv). The resulting

dx.doi.org/10.1021/ic300697w | *Inorg. Chem.* 2012, 51, 10158−10168

solution was refluxed at 65 °C for 16 h under inert atmosphere. After cooling to room temperature, the organic solution was washed with a 1 M NaOH solution (3 × 20 mL) to remove the excess cyclen and then with water (3 × 10 mL), dried over $MgSO_4$, filtered, and the solvent removed under vacuum to yield a colorless oil (0.540 g, 2.5 mmol, 87%). ^{1}H NMR (400 MHz, $CDCl_3$): δ = 2.69−2.35 (16H, m, cyclen CH_2), 2.28 (2H, t, J = 7.1 Hz, $NC\underline{H}_2$), 1.40 (2H, m, $NCH_2C\underline{H}_2$), 0.81 (3H, t, J = 7.2 Hz, $NCH_2CH_2C\underline{H}_3$); ^{13}C NMR (100 MHz, $CDCl_3$): δ = 56.3, 51.5, 46.9, 46.1, 45.1, 20.4, 12.0. ES-MS (ES+) Calculated for $C_{11}H_{27}N_4$ $[M+H]^+$: m/z = 215.2230, found: m/z = 215.2234. IR υ_{max} (cm^{-1}): 3385−3234 (m, N−H stretch), 2956−2933 (m, aliphatic C−H stretch), 1465 (s, alkane $-CH_2-$ bending), 1450−1350 (s, alkane $-CH_3-$ bending)

2,2′,2″-(10-Propyl-1,4,7,10-tetraazacyclododecane-1,4,7-triyl)tris(*N*,*N*-dimethylacetamide) (2). **1** (0.410 g, 1.9 mmol, 1.0 equiv), 2-chloro-*N*,*N*-dimethylacetamide (0.710 g, 5.9 mmol, 3.1 equiv), KI (1.010 g, 6.6 mmol, 3.5 equiv), and K_2CO_3 (0.910 g, 6.6 mmol, 3.5 equiv) were dissolved in acetonitrile (50 mL). The solution was refluxed at 83 °C for 5 days, then filtered and the solvent was removed under reduced pressure. The resulting product was redissolved in $CHCl_3$, filtered, and the solvent removed once more under reduced pressure. Purification was achieved by alumina column chromatography using a gradient elution 100 to 80:20 CH_2Cl_2:CH_3OH. The desired product was obtained as a white solid (0.54 g, 1.15 mmol, 61%). ^{1}H NMR (400 MHz, $CDCl_3$): δ = 3.50−2.05 (42H, m, cyclen $8CH_2$, $6CH_3$, $4CH_2$), 1.42 (2H, m, $NCH_2C\underline{H}_2$), 0.83 (3H, t, J = 7.1−7.2 Hz, $NCH_2CH_2C\underline{H}_3$); ^{13}C NMR (100 MHz, $CDCl_3$): δ = 170.9, 170.5, 56.1, 55.4, 55.1, 50.2, 36.8, 36.6, 35.9, 35.5, 19.2, 11.8. ES-MS (ES^+) Calculated for $C_{23}H_{48}N_7O_3$ $[M+H]^+$: m/z = 470.3813, found: m/z = 470.3818. IR υ_{max} (cm^{-1}): 2960 (s, alkane, C−H stretch), 1644 (s, amide C═O stretch), 1100 (m, CO stretch).

Complex 2·Yb. Ligand **2** (0.122 g, 0.3 mmol, 1 equiv) and $Yb(CF_3SO_3)_3$ (0.161 g, 0.3 mmol, 1.0 equiv) were dissolved in methanol (7 mL) and reacted using microwave irradiation for 40 min. The solvent was evaporated under reduced pressure to give a solid, which was dissolved in a minimal amount of methanol (3 mL) and precipitated out of swirling ether (200 mL) to give a slightly yellow powder (0.230 g, 0.2 mmol, 81%). The resulting powder was then redissolved in water, where ammonia was added until reaching pH ∼10 to eliminate the possible presence of unreacted Yb(III) triflate salt via the precipitation of its corresponding metal hydroxides. After centrifugation and microfiltration, the solution was finally brought back to pH 6−7 using dilute HCl.[43] ^{1}H NMR (400 MHz, CD_3OD): δ = 139.99, 118.06, 81.10, 39.64, 14.74, 3.00, 2.97, 1.18, 0.96, −4.12, −12.87, −22.19, −31.16, −60.56, −71.17, −93.88, −147.85. MALDI (LD^+) Calculated for $C_{24}H_{46}N_7O_6S_1F_3Yb$ $[M - H + CF_3SO_3]^+$: m/z = 791.2573, found: m/z = 791.2571. IR υ_{max} (cm^{-1}): 2940 (s, alkane, C−H stretch), 1624 (s, amide CO stretch), 1028 (m, CO stretch); CHN elemental analysis: Calculated for **2·Yb**·$3CH_2Cl_2$·$NH_4CF_3SO_3$: C, 23.83, H, 3.80, N, 7.41; Found for **2·Yb**: C, 24.34, H, 3.72, N, 7.35.

Photophysical Measurements. Otherwise stated, all measurements were performed at 298 K in HEPES buffer at pH 7.4, while the ionic strength was kept constant by the addition of NaCl (0.1 M). UV−visible absorption spectra were measured in 1-cm quartz cuvettes on a Varian Cary 50 spectrophotometer. Baseline correction was applied for all spectra. Emission (Fluorescence, phosphorescence, and excitation) spectra were recorded on a Varian Cary Eclipse Fluorimeter. Quartz cells with a 1 cm path length from Hellma were used for these measurements. The temperature was kept constant throughout the measurements by using a thermostatted unit block. Fluorescence spectra in the near-infrared range were recorded on a Fluorolog FL 3-22 spectrophotometer from Horiba Jobin Yvon with double grating emission and excitation monochromators, and a R5509-73 photomultiplier. Light intensity was measured by a C9940-22 detector from Hamamatsu (range 800−1700 nm) cooled to 77 K and coupled to a Jobin Yvon SpectrAcq v5.20 data acquisition system. Quantum yield (Q^L_{Ln}) of the **2·Yb·8-HQS** ternary complex (2×10^{-4}−5×10^{-5} M) has been determined in HEPES buffer (pH 7.4), relative to the quantum yield of $[Yb(tta)_3phen]$ (tta = thenoyltrifluoroacetylacetonate; phen = 1,10-phenanthroline) in toluene, Q^L_{Ln} = 1.10%,[36] at 298 K.

Spectrophotometric Titrations and Binding Constants. The formation of the luminescent 1:1 ternary complex, **2·Yb·8-HQS**, was ascertained by both UV−visible and luminescence titrations of a solution of **2·Yb** ($1-5 \times 10^{-5}$ M) with **8-HQS** (0→5 equiv). The data were fitted using the nonlinear regression analysis program, SPECFIT.[44]

The **2·Yb·8-HQS** system was then titrated with alkaline earth and transition metals (0→10 equiv). In a typical experiment, 1 equiv of **8-HQS** was added prior titration to a 2.7 mL HEPES-buffered solution of **2·Yb** 5×10^{-5} M. After each metal addition, UV−visible, emission in both visible and NIR ranges and excitation spectra were recorded at 298 K. For the titration of the ternary complex as a function of pH, 25 mL of a 5×10^{-5} M **2·Yb** solution in the presence of 1 equiv of **8-HQS** was first acidified by adding a drop of HCl 37% to reach pH 2−2.5 and then titrated with freshly prepared sodium hydroxide solutions at different concentrations (1, 0.1, and 0.01 M). After each addition of base, the pH of the solution was measured using a KCl-saturated electrode from Metrohm AG and UV−visible absorption and emission (both visible and NIR) spectra were recorded.

■ ASSOCIATED CONTENT

Supporting Information

^{1}H NMR and IR of **2·Yb**; stability constants for the formation of the 1:1 ternary complex **2·Yb·8-HQS**, and evidence for the sensitization of the Yb(III)-centered emission via the **8-HQS** antenna including UV−visible absorption, emission, and excitation spectra; effect of the pH or the addition of Cd(II), Fe(II), Co(II), Ni(II), and Cu(II) on the photophysical properties of **2·Yb·8-HQS**; influence of Ca(II) and Mg(II) on the NIR emission of **2·Yb·8-HQS** and detection of Zn(II); changes observed in the UV−visible absorption spectrum of **2·Yb·8-HQS** during the reversibility experiment using EDTA. This material is available free of charge via the Internet at http://pubs.acs.org.

■ AUTHOR INFORMATION

Corresponding Author

*E-mail: combys7@gmail.com (S.C.), gunnlaut@tcd.ie (T.G.).

Notes

The authors declare no competing financial interest.

■ ACKNOWLEDGMENTS

The authors thank Prof. S. Faulkner and Dr. T. J. Sorensen at Oxford University for the NIR lifetime measurements, as well as Science Foundation Ireland (RFP 2008 and 2009), The Irish Research Council for Science, Engineering & Technology (IRCSET) (L.T., O.K.) and the Swiss National Science Foundation (SNSF) (S.C.) for funding.

■ REFERENCES

(1) (a) McRae, R.; Bagchi, P.; Sumalekshmy, S.; Fahrni, C. J. *Chem. Rev.* **2009**, *109*, 4780−4827. (b) Que, E. L.; Domaille, D. W.; Chang, C. J. *Chem. Rev.* **2008**, *108*, 1517. (c) Quang, D. T.; Kim, J. S. *Chem. Rev.* **2010**, *110*, 6280. (d) Lodeiro, C.; Capelo, J. L.; Mejuto, J. C.; Oliveira, E.; Santos, H. M.; Pedras, B.; Nunez, C. *Chem. Soc. Rev.* **2010**, *39*, 2948.

(2) (a) Burdette, S. C.; Lippard, S. J. *Coord. Chem. Rev.* **2001**, *216−217*, 333. (b) Kikuchi, K.; Komatsu, K.; Nagano, T. *Curr. Opin. Chem. Biol.* **2004**, *8*, 182. (c) Nolan, E. M.; Lippard, S. J. *Acc. Chem. Res.* **2009**, *42*, 193. (d) Ghosh, S. K.; Kim, P.; Zhang, X. a.; Yun, S. H.; Moore, A.; Lippard, S. J.; Medarova, Z. *Cancer Res.* **2010**, *70*, 6119. (e) Pluth, M. D.; Tomat, E.; Lippard, S. J. *Annu. Rev. Biochem.* **2011**, *80*, 333.

(3) Kelleher, S. L.; McCormick, N. H.; Velasquez, V.; Lopez, V. *Adv. Nutr.* **2011**, *2*, 101.
(4) (a) Frederickson, C. J.; Koh, J. Y.; Bush, A. I. *Nat. Rev. Neurosci.* **2005**, *6*, 449. (b) Sensi, S. L.; Paoletti, P.; Bush, A. I.; Sekler, I. *Nat. Rev. Neurosci.* **2009**, *10*, 780.
(5) (a) Rink, L. *Proc. Nutr. Soc.* **2000**, *59*, 541. (b) Fraker, P. J.; King, L. E. *Annu. Rev. Nutr.* **2004**, *24*, 277.
(6) Fukada, T.; Yamasaki, S.; Nishida, K.; Murakami, M.; Hirano, T. *J. Biol. Inorg. Chem.* **2011**, *16*, 1123.
(7) Costello, L.; Franklin, R. *Mol. Cancer* **2006**, *5*, 17.
(8) (a) Sensi, S. L.; Paoletti, P.; Koh, J. Y.; Aizenman, E.; Bush, A. I.; Hershfinkel, M. *J. Neurosci.* **2011**, *31*, 16076. (b) Gh Popescu, B. F.; Nichol, H. *CNS Neurosci. Ther.* **2011**, *17*, 256.
(9) (a) Xu, Z.; Yoon, J.; Spring, D. R. *Chem. Soc. Rev.* **2010**, *39*, 1996. (b) Jiang, P.; Guo, Z. *Coord. Chem. Rev.* **2004**, *248*, 205. (c) Buccella, D.; Horowitz, J. A.; Lippard, S. J. *J. Am. Chem. Soc.* **2011**, *133*, 4101. (d) Chen, M.; Lv, X.; Liu, Y.; Zhao, Y.; Liu, J.; Wang, P.; Guo, W. *Org. Biomol. Chem.* **2011**, *9*, 2345. (e) Kuang, G. C.; Allen, J. R.; Baird, M. A.; Nguyen, B. T.; Zhang, L.; Morgan, T. J.; Levenson, C. W.; Davidson, M. W.; Zhu, L. *Inorg. Chem.* **2011**, *50*, 10493. (f) Liu, T.; Liu, S. *Anal. Chem.* **2011**, *83*, 2775. (g) Sun, F.; Zhang, G.; Zhang, D.; Xue, L.; Jiang, H. *Org. Lett.* **2011**, *13*, 6378. (h) He, C.; Zhu, W.; Xu, Y.; Zhong, Y.; Zhou, J.; Qian, X. *J. Mater. Chem.* **2010**, *20*, 10755.
(10) (a) Parkesh, R.; Clive Lee, T.; Gunnlaugsson, T. *Org. Biomol. Chem.* **2007**, *5*, 310. (b) Lu, C.; Xu, Z.; Cui, J.; Zhang, R.; Qian, X. *J. Org. Chem.* **2007**, *72*, 3554. (c) Qian, X.; Xiao, Y.; Xu, Y.; Guo, X.; Qian, J.; Zhu, W. *Chem. Commun.* **2010**, *46*, 6418. (d) Tamanini, E.; Flavin, K.; Motevalli, M.; Piperno, S.; Gheber, L. A.; Todd, M. H.; Watkinson, M. *Inorg. Chem.* **2010**, *49*, 3789. (e) Jobe, K.; Brennan, C. H.; Motevalli, M.; Goldup, S. M.; Watkinson, M. *Chem. Commun.* **2011**, *47*, 6036. (f) Xu, Z.; Baek, K. H.; Kim, H. N.; Cui, J.; Qian, X.; Spring, D. R.; Shin, I.; Yoon, J. *J. Am. Chem. Soc.* **2009**, *132*, 601.
(11) (a) Tomat, E.; Lippard, S. J. *Inorg. Chem.* **2010**, *49*, 9113. (b) Bazzicalupi, C.; Bencini, A.; Biagini, S.; Faggi, E.; Farruggia, G.; Andreani, G.; Gratteri, P.; Prodi, L.; Spepi, A.; Valtancoli, B. *Dalton Trans.* **2010**, *39*, 7080. (c) Li, D.; Chen, S.; Bellomo, E. A.; Tarasov, A. I.; Kaut, C.; Rutter, G. A.; Li, W. H. *Proc. Natl. Acad. Sci. U.S.A.* **2011**, *108*, 21063.
(12) (a) Koutaka, H.; Kosuge, J. i.; Fukasaku, N.; Hirano, T.; Kikuchi, K.; Urano, Y.; Kojima, H.; Nagano, T. *Chem. Pharm. Bull.* **2004**, *52*, 700. (b) Wu, Y.; Peng, X.; Guo, B.; Fan, J.; Zhang, Z.; Wang, J.; Cui, A.; Gao, Y. *Org. Biomol. Chem.* **2005**, *3*, 1387. (c) Ulrich, G.; Ziessel, R.; Harriman, A. *Angew. Chem., Int. Ed.* **2008**, *47*, 1184.
(13) (a) Gunnlaugsson, T.; Lee, T. C.; Parkesh, R. *Org. Lett.* **2003**, *5*, 4065. (b) Cao, S.; Li, H.; Chen, T.; Chen, J. *J. Solution Chem.* **2009**, *38*, 1520. (c) Ghosh, K.; Saha, I. *Tetrahedron Lett.* **2010**, *51*, 4995. (d) Gunnlaugsson, T.; Bichell, B.; Nolan, C. *Tetrahedron* **2004**, *60*, 5799. (e) Gunnlaugsson, T.; Bichell, B.; Nolan, C. *Tetrahedron Lett.* **2002**, *43*, 4989.
(14) (a) Zhao, Q.; Li, F.; Huang, C. *Chem. Soc. Rev.* **2010**, *39*, 3007. (b) Zhao, Q.; Huang, C.; Li, F. *Chem. Soc. Rev.* **2011**, *40*, 2508. (c) Lee, P. K.; Law, W. H.-T.; Liu, H. W.; Lo, K. K.-W. *Inorg. Chem.* **2011**, *50*, 8570. (d) You, Y.; Lee, S.; Kim, T.; Ohkubo, K.; Chae, W. S.; Fukuzumi, S.; Jhon, G. J.; Nam, W.; Lippard, S. J. *J. Am. Chem. Soc.* **2011**, *133*, 18328.
(15) (a) Reany, O.; Gunnlaugsson, T.; Parker, D. *Chem. Commun.* **2000**, 473. (b) Reany, O.; Gunnlaugsson, T.; Parker, D. *J. Chem. Soc., Perkin Trans. 2* **2000**, 1819.
(16) (a) Pope, S. J. A.; Laye, R. H. *Dalton Trans.* **2006**, 3108. (b) Andrews, M.; Jones, J. E.; Harding, L. P.; Pope, S. J. A. *Chem. Commun.* **2011**, *47*, 206. (c) Ye, Z.; Wang, G.; Chen, J.; Zhang, W.; Yuan, J. *Biosens. Bioelectron.* **2010**, *26*, 1043.
(17) (a) Hanaoka, K.; Kikuchi, K.; Kojima, H.; Urano, Y.; Nagano, T. *Angew. Chem., Int. Ed.* **2003**, *42*, 2996. (b) Hanaoka, K.; Kikuchi, K.; Kojima, H.; Urano, Y.; Nagano, T. *J. Am. Chem. Soc.* **2004**, *126*, 12470. (c) Hanaoka, K.; Kikuchi, K.; Kobayashi, S.; Nagano, T. *J. Am. Chem. Soc.* **2007**, *129*, 13502. (d) Hanaoka, K. *Chem. Pharm. Bull.* **2010**, *58*, 1283.
(18) (a) Kotova, O.; Comby, S.; Gunnlaugsson, T. *Chem. Commun.* **2011**, *47*, 6810. (b) McMahon, B. K.; Gunnlaugsson, T. *Tetrahedron Lett.* **2010**, *51*, 5406. (c) Nonat, A. M.; Harte, A. J.; Sénéchal-David, K.; Leonard, J. P.; Gunnlaugsson, T. *Dalton Trans.* **2009**, 4703. (d) Gunnlaugsson, T.; Harte, A. J.; Leonard, J. P.; Senegal, K. *Chem. Commun.* **2004**, 782. (e) Andrews, M.; Jones, J. E.; Harding, L. P.; Pope, S. J. A. *Chem. Commun.* **2011**, *47*, 206. (f) Thibon, A.; Pierre, V. C. *J. Am. Chem. Soc.* **2009**, *131*, 434.
(19) (a) dos Santos, C. M. G.; Harte, A. J.; Quinn, S. J.; Gunnlaugsson, T. *Coord. Chem. Rev.* **2008**, *252*, 2512. (b) Leonard, J. P.; Nolan, C. B.; Stomeo, F.; Gunnlaugsson, T. *Top. Curr. Chem.* **2007**, *281*, 1. (c) Bünzli, J.-C. G.; Chauvin, A.-S.; Vandevyver, C. D. B.; Song, B.; Comby, S. *Ann. N.Y. Acad. Sci.* **2008**, *1130*, 97. (d) Moore, E. G.; Samuel, A. P. S.; Raymond, K. N. *Acc. Chem. Res.* **2009**, *42*, 542. (e) Bünzli, J. C. *Chem. Rev.* **2010**, *110*, 2729. (f) Parker, D. *Aust. J. Chem.* **2011**, *64*, 239. (g) Thibon, A.; Pierre, V. C. *Anal. Bioanal. Chem.* **2009**, *394*, 107.
(20) Comby, S.; Bünzli, J.-C. G. Lanthanide Near-Infrared Luminescence in Molecular Probes and Devices. In *Handbook on the Physics and Chemistry of Rare Earths*; Gschneidner, K. A., Jr., Bünzli, J.-C. G., Pecharsky, V. K., Eds.; Elsevier Science B.V.: Amsterdam, The Netherlands, 2007; Vol. *37*, pp 217−470.
(21) (a) Nonat, A. M.; Quinn, S. J.; Gunnlaugsson, T. *Inorg. Chem.* **2009**, *48*, 4646. (b) Nonat, A. M.; Allain, C.; Faulkner, S.; Gunnlaugsson, T. *Inorg. Chem.* **2010**, *49*, 8449. (c) Shinoda, S.; Tsukube, H. *Analyst* **2011**, *136*, 431. (d) Moore, E. G.; Xu, J.; Dodani, S. C.; Jocher, C. J.; D'Aléo, A.; Seitz, M.; Raymond, K. N. *Inorg. Chem.* **2010**, *49*, 4156. (e) An, J.; Shade, C. M.; Chengelis-Czegan, D. A.; Petoud, S.; Rosi, N. L. *J. Am. Chem. Soc.* **2011**, *133*, 1220. (f) Zhang, T.; Zhu, X.; Cheng, C. C. W.; Kwok, W. M.; Tam, H. L.; Hao, J.; Kwong, D. W. J.; Wong, W. K.; Wong, K. L. *J. Am. Chem. Soc.* **2011**, *133*, 20120. (g) Zhong, Y.; Si, L.; He, H.; Sykes, A. G. *Dalton Trans.* **2011**, *40*, 11389.
(22) Weissleder, R.; Ntziachristos, V. *Nat. Med.* **2003**, *9*, 123.
(23) Mahmood, U.; Weissleder, R. *Mol. Cancer Ther.* **2003**, *2*, 489.
(24) (a) Leonard, J. P.; dos Santos, C. M. G.; Plush, S. E.; McCabe, T.; Gunnlaugsson, T. *Chem. Commun.* **2007**, 129. (b) Massue, J.; Quinn, S. J.; Gunnlaugsson, T. *J. Am. Chem. Soc.* **2008**, *130*, 6900. (c) Murray, N. S.; Jarvis, S. P.; Gunnlaugsson, T. *Chem. Commun.* **2009**, *33*, 4959. (d) Comby, S.; Gunnlaugsson, T. *ACS Nano* **2011**, *5*, 7184.
(25) (a) Gillin, W. P.; Curry, R. J. *Appl. Phys. Lett.* **1999**, *74*, 798. (b) Nonat, A.; Imbert, D.; Pécaut, J.; Giraud, M.; Mazzanti, M. *Inorg. Chem.* **2009**, *48*, 4207. (c) Tallec, G.; Fries, P. H.; Imbert, D.; Mazzanti, M. *Inorg. Chem.* **2011**, *50*, 7943.
(26) (a) Comby, S.; Imbert, D.; Chauvin, A.-S.; Bünzli, J.-C. G. *Inorg. Chem.* **2006**, *45*, 732. (b) Comby, S.; Gumy, F.; Bünzli, J.-C. G.; Saraidarov, T.; Reisfeld, R. *Chem. Phys. Lett.* **2006**, *432*, 128. (c) Comby, S.; Imbert, D.; Vandevyver, C. D. B.; Bünzli, J.-C. G. *Chem.—Eur. J.* **2007**, *13*, 936.
(27) (a) Albrecht, M.; Fröhlich, R.; Bünzli, J.-C. G.; Aebischer, A.; Gumy, F.; Hamacek, J. *J. Am. Chem. Soc.* **2007**, 14178. (b) Albrecht, M.; Fiege, M.; Osetska, O. *Coord. Chem. Rev.* **2008**, *252*, 812. (c) Albrecht, M.; Osetska, O.; Bünzli, J.-C. G.; Gumy, F.; Fröhlich, R. *Chem.—Eur. J.* **2009**, *15*, 8791.
(28) Mahanand, D.; Houck, J. C. *Clin. Chem.* **1968**, *14*, 6.
(29) Martell, A. E.; Smith, R. M. *Critical Stability Constants*; Plenum Press: New York, 1975; Vol. *2*, pp 223−227.
(30) Massue, J.; Plush, S. E.; Bonnet, C. S.; Moore, D. A.; Gunnlaugsson, T. *Tetrahedron Lett.* **2007**, *48*, 8052.
(31) Serratrice, G.; Boukhalfa, H.; Beguin, C.; Baret, P.; Caris, C.; Pierre, J.-L. *Inorg. Chem.* **1997**, *36*, 3898.
(32) Launay, F.; Alain, V.; Destandau, E.; Ramos, N.; Bardez, E.; Baret, P.; Pierre, J. L. *New J. Chem.* **2001**, *25*, 1269.
(33) Faulkner, S.; Beeby, A.; Carrié, M.-C.; Dadabhoy, A.; Kenwright, A. M.; Sammes, P. G. *Inorg. Chem. Commun.* **2001**, *4*, 187.
(34) Strasser, A.; Vogler, A. *Inorg. Chim. Acta* **2004**, *357*, 2345.
(35) Artizzu, F.; Mercuri, M. L.; Serpe, A.; Deplano, P. *Coord. Chem. Rev.* **2011**, *255*, 2514.

(36) Meshkova, S. B.; Topilova, Z. M.; Bolshoi, D. V.; Beltyukova, S. V.; Tsvirko, M. P.; Venchikov, V. Y. *Acta Phys. Pol., A* **1999**, *95*, 983.
(37) (a) Shavaleev, N. M.; Adams, H.; Best, J.; Edge, R.; Navaratnam, S.; Weinstein, J. A. *Inorg. Chem.* **2006**, *45*, 9410. (b) Kunkely, H.; Vogler, A. *Inorg. Chim. Acta* **2009**, *362*, 196. (c) Hallett, A. J.; Pope, S. J. A. *Inorg. Chim. Acta* **2012**, *387*, 145.
(38) Valeur, B. *Molecular Fluorescence: Principles and Applications*; Wiley-VCH Verlag GmbH: Weinheim, Germany, 2001.
(39) Bardez, E.; Devol, I.; Larrey, B.; Valeur, B. *J. Phys. Chem. B* **1997**, *101*, 7786.
(40) Plush, S. E.; Clear, N. A.; Fanning, A.-M.; Leonard, J. P.; Gunnlaugsson, T. *Dalton Trans.* **2010**, *39*, 3644.
(41) Le Bahers, T.; Adamo, C.; Ciofini, I. *J. Phys. Chem. A* **2010**, *114*, 5932.
(42) Claus, A.; Posselt, M., XLVIII *J. Prakt. Chem.* **1890**, *41*, 32.
(43) Law, G. L.; Man, C.; Parker, D.; Walton, J. W. *Chem. Commun.* **2010**, *46*, 2391.
(44) (a) Gampp, H.; Maeder, M.; Meyer, C. J.; Zuberbühler, A. D. *Talanta* **1985**, *32*, 95. (b) Gampp, H.; Maeder, M.; Meyer, C. J.; Zuberbühler, A. D. *Talanta* **1986**, *33*, 943.